ISSN 1 746-7233, England, UK
World Journal of Modelling and Simulation
Vol. 14 (2018) No. 1, pp. 21-29

Optimization of the Flow-induced Crystallization Viscoelastic Melt Spinning Processes with respect to Processing Conditions

SSN Perera[1*]

Research & Development Centre for Mathematical Modeling, Faculty of Science, University of Colombo, Colombo 03, Sri Lanka

(*Received February 25 2017, Accepted September 26 2017*)

Abstract. The melt spinning process for artificial fibers has been studied by many research groups throughout the world during the last four decades. All these works have considered the forward problem of simulating the process for a given set of parameters. Optimization of the viscoelastic melt spinning process, especially flow-induced crystallization with respect to processing conditions has not yet been discussed in the literature. In this study, an optimization problem for a mathematical model of a flow-induced crystallization viscoelastic melt spinning process is considered with the aim of obtaining a final spinline temperature below the fiber solidification temperature. The Maxwell-Oldroyd model is used to describe the rheology of the polymeric material, the fiber is made of. The extrusion velocity of the polymer at the spinneret as well as the velocity and temperature of the quench air and fiber length serve as control variables. By defining the cost functional, the optimization problem is converted into the constrained optimization problem and the first order optimality system is derived. We propose the steepest descent algorithm based on the adjoint variable method for the numerical simulation. A computer program in MATLAB is developed for the numerical simulations.

Keywords: fiber spinning, first-order optimality system, adjoint system, steepest descent algorithm

1 Introduction

The fiber spinning process is used to make all types of synthetic textile fibers (nylon, polyester, rayon, etc.). In the melt-spinning version of the process, molten polymer is extruded through a die called a spinneret to create a thin cylinder (see Fig.1). Far away from the spinneret, the fiber is wrapped around a drum, which pulls it away at a pre-determined take-up speed. The take-up speed (around 50 m/s) is much higher than the extrusion speed (around 10 m/s)[4, 8], so the filament is stretched considerably in length, and decreases in diameter. The ambient atmosphere temperature is below the polymer solidification temperature, and therefore the polymer is cooled and solidifies before the take-up. In industrial processes a whole bundle of hundreds of single filaments is extruded and spun in parallel. However for the analysis we consider a single filament.

The dynamics of melt spinning processes has been studied by many research groups throughout the world during the last decades starting with the early works of Kase and Matsuo[6] and Ziabicki[13] . In later works, the energy balance for the heat transfer was introduced into the model, and more and more sophisticated descriptions, including material effects, crystallization kinetics and viscoelastic behavior, were developed by several authors in order to achieve a better understanding of the fiber formation process. Up to now it has been possible to use the basic models with slight modifications in different technological aspects of the melt spinning process. Due to the complex behaviour of the polymeric material, several parameters are included in all the available models. The outcome of the melt spinning process depends heavily on the boundary conditions / external variables, e.g., the draw ratio, the ambient temperature, the quench air velocity and the temperature. Therefore the

* Corresponding author. *E-mail address*: ssnp@maths.cmb.ac.lk

sensitivity and optimization of the melt spinning process with respect to processing conditions and material constants are important. The subject of sensitivity and optimization of melt spinning processes was reported in the literature without the crystallization process[1–3, 9, 10, 12] . However, the subject of optimizing the flow induced crystallization viscoelastic melt spinning process with respect to the external variables has not yet been treated in the literature.

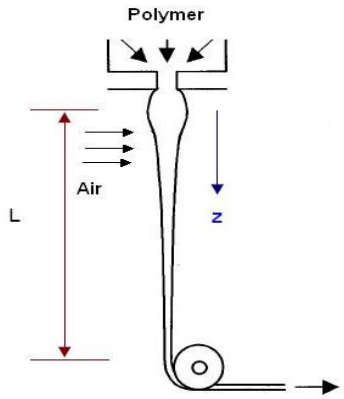

Fig. 1: Sketch of the melt spinning process

The main goal of this study is to control the temperature profile of the fiber, such that the final temperature is below the fiber solidification point. We consider the Maxwell-Oldroyd model to describe the rheology of the polymeric material. We consider the optimal control problem as a constrained minimization problem[5], and derive the corresponding first-order optimality system via the Lagrange functional. For the numerical computation of the optimal control variables, a steepest descent algorithm is presented using the adjoint variables.

2 Optimization problem

2.1 Melt spinning model

By considering the basic conservation laws for the mass, momentum and energy of the viscous polymer jet, one can obtain the following set of equations[3, 6, 8, 10] by averaging over the cross–section of the slender fiber.

$$\rho A v \;=\; W_0, \tag{1a}$$

$$\rho A v \frac{dv}{dz} \;=\; \frac{dA\tau}{dz} \;+\; \rho A g - \sqrt{A\pi} C_d \rho_{air} v^2, \tag{1b}$$

$$\rho C_p v \frac{dT}{dz} \;=\; -\frac{2\alpha\sqrt{\pi}}{\sqrt{A}} (T \;-\; T_a) + \rho \Delta H v \frac{d\varphi}{dz} \tag{1c}$$

$$v\frac{d\varphi}{dz} = K_{\max}(\varphi_\infty - \varphi) \exp\left[-4\ln 2\left(\frac{T - T_{\max}}{D}\right)^2 + \left(\frac{\varsigma}{G_0}\right)\tau\right] \tag{1d}$$

Here A denotes the spinline cross-sectional area, ρ is the density of the fluid, g is the gravity, W_0 is the mass throughput, v is the spinline velocity, z is the distance coordinate from the spinneret, T represents the spinline temperature, T_0 is the initial temperature, T_a is the air temperature, C_p is the fluid heat capacity, ΔH is the specific heat of fusion of a perfect crystal and α denotes the heat transfer coefficient. In equation (1d) φ is the crystalline index,φ_∞ denotes the ultimate crystallinity, K_{max} is the maximum crystallization rate, T_{max} is the fluid temperature having the maximum crystallization rate, D denotes the crystallization half width

temperature range, G_0 is the fluid shear modulus and ζ denotes the flow-induced crystallization enhancement factor. The spinline axial stress τ is given by the Maxwell-Oldroyd equation:

$$\tau + \lambda\left(v\frac{d\tau}{dz} - 2\tau\frac{dv}{dz}\right) = 3\eta\frac{dv}{dz}. \tag{1e}$$

Here τ and λ denote the viscosity and the fluid characteristic relaxation time respectively and are given by

$$\eta = \eta_0 \exp\left[\frac{E_a}{R_G}\left(\frac{1}{T} - \frac{1}{T_0}\right) + \vartheta\frac{\varphi}{\varphi_\infty}\right], \lambda = \lambda_0 \exp\left[\frac{E_a}{R_G}\left(\frac{1}{T} - \frac{1}{T_0}\right) + (\vartheta - 3.2)\frac{\varphi}{\varphi_\infty}\right] \tag{1f}$$

where E_a denotes the activation energy, R_G equals the gas constant, η_0 is the zero shear viscosity at the initial temperature T_0 and λ_0 denotes η_0/G_0 , and ϑ is the model parameter representing the crystallinity dependence of the viscosity. We assume the following relation for the heat transfer coefficient [8]

$$\alpha = \frac{0.21}{R_0}\kappa \mathrm{Re}_{\mathrm{air}}^{\frac{1}{3}}\left[1 + \frac{64v_c^2}{v^2}\right]^{\frac{1}{6}} \tag{1g}$$

and air drag coefficient

$$C_d = 0.37\mathrm{Re}_{air}^{-0.61} \tag{1h}$$

depending on the Reynolds-number of the quench air flow

$$\mathrm{Re}_{\mathrm{air}} = \frac{2v\rho_{\mathrm{air}}}{\eta_{\mathrm{air}}}\sqrt{\frac{A}{\pi}}. \tag{1i}$$

Here R_0 is the radius of the spinneret, ρ_{air},η_{air} and κ represent respectively the density, viscosity and heat conductivity of the air and ν_c is the velocity of the quench air.

The equations (1a)-(1d) are subject to the boundary conditions

$$v = v_0, T = T_0, \varphi = 0 \text{ at } z = 0, \text{ and } v = v_L \text{ at } z = L \tag{1j}$$

where L denotes the length of the spinline.

The dimensional equations of (1) are now rendered into dimensionless form by introducing the following quantities $z^* = \frac{z}{L}, v^* = \frac{v}{v_0}, T^* = \frac{T}{T_0}, q^* = \frac{q}{q_0}, A^* = \frac{A}{A_0}$ and $\varphi^* = \frac{\varphi}{\varphi_\infty}$, where $q = \rho A\tau/W_0$ and $q_0 = \rho A_0 v_0\eta_0/LW_0$. Dropping the star, and rearranging the terms, the system reads as

$$\frac{dv}{dz} = \frac{1}{3\eta + \mathrm{De}vq}\left(qv + \mathrm{De}v^2\frac{dq}{dz}\right) \tag{2a}$$

$$\frac{dq}{dz} = \mathrm{Re}\left(\frac{dv}{dz} - \frac{\mathrm{Fr}^{-1}}{v} + C_1 v^{3/2}\right) \tag{2b}$$

$$\frac{dT}{dz} = -C_2\frac{(T - T_a)}{\sqrt{v}} + \frac{\Delta H\varphi_\infty}{T_0 C_p}\frac{d\varphi}{dz} \tag{2c}$$

$$\frac{d\varphi}{dz} = \frac{K_{\max} L}{v_0}\left(\frac{1-\varphi}{v}\right)\exp\left[-4\ln 2\left(\frac{T-T_{\max}}{D}\right)^2 + C_3\tau\right] \tag{2d}$$

where $R_e = \rho L v_0/\eta_0$ is the Reynolds number, $Fr^{-1} = gL/v_0$ is the inverse of the Froude number, $C_1 = C_d\rho_{air}L\sqrt{\pi}/\rho\sqrt{A_0}$ is the scaled drag coefficient, $C_2 = 2\alpha L\sqrt{\pi}/\rho C_p v_0\sqrt{A_0}$ denotes the scaled heat transfer coefficient and $C_3 = \varsigma\eta_0 v_0/G_0 L$. The viscosity and Deborah number are given by

$$\eta = \exp\left[\frac{E_a}{R_G T_0}\left(\frac{1}{T} - 1\right) + \vartheta\varphi\right],\ \mathrm{De} = \frac{\lambda_0 v_0}{L}\exp\left[\frac{E_a}{R_G T_0}\left(\frac{1}{T} - 1\right) + (\vartheta - 3.2)\varphi\right]. \tag{2e}$$

The boundary conditions read as

$$v(0) = 1, v(1) = d, T(0) = 1, \varphi(0) = 0. \tag{2f}$$

2.2 Cost functional

The temperature profile of the fiber needs to be controlled, such that the final temperature is below the fiber solidification point$T_s^* = T_s/T_0$ The air temperature T_a, the air velocity v_c, the extrusion velocity v_0 and the fiber length L can be influenced and hence serve as control variables. Therefore, we consider the following two cost functionals

$$\begin{aligned} J_1 = &-\omega_1 u_3 + \omega_2(y_3(1) - T_s^*) + \tfrac{\omega_3}{2}\int_0^1 (u_2(z) - T_{ref})^2 dz \\ &+ \tfrac{\omega_4}{2}\int_0^1 u_1(z)^2 dz - \tfrac{\omega_5}{2}\int_0^1 (\varphi(z) - \varphi_d)^2 dz \end{aligned} \tag{3a}$$

$$\begin{aligned} J_2 = &-\omega_1 u_3 + \omega_2(y_3(1) - T_s^*) + \tfrac{\omega_3}{2}\int_0^1 (u_2(z) - T_{ref})^2 dz + \tfrac{\omega_4}{2}\int_0^1 u_1(z)^2 dz \\ &- \tfrac{\omega_5}{2}\int_0^1 (\varphi(z) - \varphi_d)^2 dz + \tfrac{\omega_6}{2}\int_0^1 u_4(z)^2 dz \end{aligned} \tag{3b}$$

where T_{ref} denotes the reference temperature, $y = (v, q, T, \varphi) \in Y$ denotes the vector of state variables and the control variable $u \in U$ is given by $u = (v_c, T_a, v_0)$ for J_1 and $u = (v_c, T_a, v_0, L)$ forJ_2 The weighting coefficients $\omega_i > 0$, i = 1,.., 6 allow the adjustment of the cost functionals to different scenarios. Now we can consider the following constrained optimization problems

$$\mathrm{minimize} J_1(y, u)\mathrm{w.r.t.}u, \mathrm{subject\ \ to}(2) \tag{4}$$

$$\mathrm{minimize} J_2(y, u)\mathrm{w.r.t.}u, \mathrm{subject\ \ to}(2). \tag{5}$$

2.3 The first-order optimality system

In this section, we introduce the Lagrangian associated to the constrained minimization problems (4) and (5) and derive the system of first order optimality conditions. To derive the necessary theory we consider problem (4). Here, for convenience the cost functional is denoted as J. Let $y \in Y = C^1([0, 1]; R^4)$ be the state space and $u \in C^1([0, 1]; R^2) \times R$ be the control space where $y = (v, q, T, \varphi)$ and $u = (v_c, T_a, v_0)$.

The operator $e = (e_v, e_q, e_T, e_\varphi) : Y \times U \to Y^*$ is defined via the weak formulation of the state system (2): $\langle e(y, u), \xi\rangle_{Y,Y^*} = 0\ \ \forall\xi \in Y^*$ where $\langle ., .\rangle_{Y,Y^*}$ denotes the duality pairing between Y and its dual space Y^*. Now the minimization problem (4) reads as

$$\text{minimize} J(y,u) \text{w.r.t.} u \in U, \text{subject to } e(y,u) = 0. \tag{6}$$

Introducing the Lagrangian $L : Y \times U \times Y^* \to R$ defined as $L(y,u,\xi) = J(y,u) + \langle e(y,u), \xi \rangle_{Y,Y^*}$, the first-order optimality system reads as $\nabla_{y,u,\xi} L(y,u,\xi) = 0$. Taking the variation of L with respect to the adjoint variable ξ and the state variable y, one can obtain the state system and the adjoint system respectively. $\frac{\partial L}{\partial y} = 0 \Rightarrow J_y(y,u) + e_y^*(y,u)\xi = 0$. The classical form of the state system is

$$\frac{dy}{dz} = f(y,u), y_1(0) = 1, y_1(1) = d, y_3(0) = 1, y_4(0) = 0 \tag{7a}$$

where f(y,u) can be obtained by rearranging system (2). The classical form of the adjoint system is

$$\frac{d\xi}{dz} = -F(y,u,\xi), \xi_q(0) = 0, \xi_\varphi(1) = 0, \xi_T(1) = -\omega_2, \xi_\varphi(1) = 0, \text{ where } F(y,u,\xi) = \left(\frac{\partial f}{\partial y}\right)^{\mathrm{T}} \xi. \tag{7b}$$

Finally, by considering the variation of L with respect to the control variable u in the direction of δu, the optimality condition can be obtained as

$$\langle J_u(y,u), \delta u \rangle + \langle e_u(y,u)\delta u, \xi \rangle = 0. \tag{7c}$$

3 Algorithm

To solve the non-linear first order-optimality system (7), we propose an iterative steepest-descent method. The main steps of the solving algorithm are given Fig. 2

Here, Tol is some prescribed tolerance for the termination of the optimization procedure. In each iteration step, we need to solve two boundary value problems, i.e. the state system (7a) and the adjoint system (7b). Both systems are solved using a shooting method based on a Newton-iteration.

3.1 Step size control with polynomial model

Crucial for the convergence of the algorithm is the choice of the step size β in the direction of the gradient. Clearly, the best choice would be the result of a line search $\beta^* = \text{argmin}_{\beta>0} J(u^{(k)} - g^{(k)})$.

However this is numerically quite expensive although it is a one dimensional minimization problem. Instead of the exact line search method, we use an approximation based on a quadratic polynomial method [7] in order to find β^* such that which minimizes $J(u^{(k)} - \beta g^{(k)})$. We construct the quadratic polynomial for $\Phi(\beta) = J(u^{(k)}, g^{(k)})$. Using the following data points, $\Phi(0) = J(u^{(k)}), \Phi(1) = J(u^{(k)} - g^{(k)}), \Phi'(0) = \nabla J(u^{(k)})^{\mathrm{T}} g^{(k)} < 0$. Then the quadratic polynomial of β reads as follows, $\Psi(\beta) = \Phi(0) + \Phi'(0)\beta + (\Phi(1) - \Phi(0) - \Phi'(0))\beta^2$. The global minimum of ϕ is, $\beta^* = \frac{-\Phi'(0)}{2(\Phi(1)-\Phi(0)-\Phi'(0))} \in (0,1)$.

3.2 Numerics

Both state (7a) and adjoint (7b) were solved using the MATLAB routine ode23tb. This routine uses an implicit method with backward differentiation to solve stiff differential equations. It is an implementation of TR-BDF2[11], an implicit two stage Runge-Kutta formula where the first stage is a trapezoidal rule step and the second stage is a backward differentiation formula of order two.

3.3 Simulation conditions

Tab. 1 summarizes the simulation conditions and material parameter values which we used in the simulation. These values typically for Nylon-66 and are taken from[8].

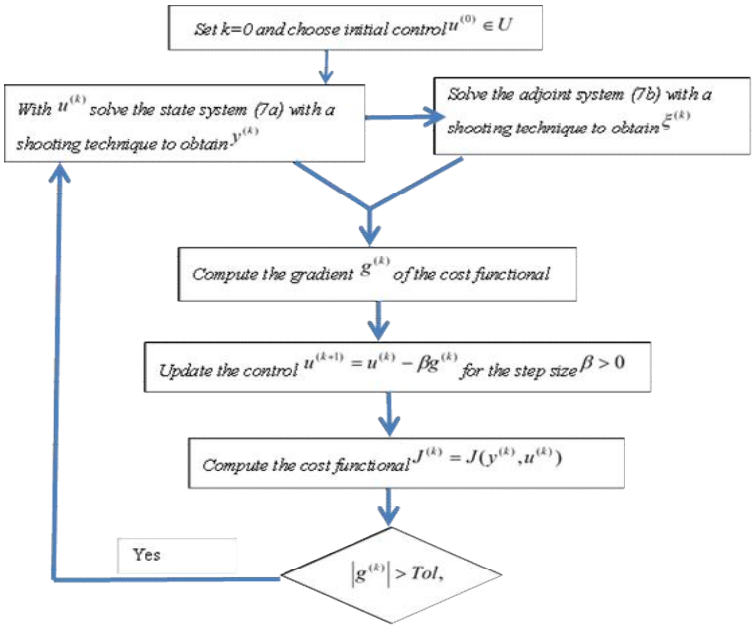

Fig. 2: Solving Algorithm

Table 1: Material parameter values

Parameter	Value	Parameter	Value
ρ	$0.98g/cm^3$	G_0	1.10^5pa
C_p	$0.46cal/(g°C$	$T_{(Melting\ \ temperature)}$	$260°C$
T_0	$300°C$	ΔH	$148J/g$
ρ_{air}	$1.189Kg/m^3$	K_{max}	$0.55s^{-1}$
η_{air}	$1.1819 \cdot 10^{-5}pas$	T_{max}	$150°C$
E_a	$13500cal/mol$	D	$60°C$
η_0 at $280°C$	$163pas$	ζ	8.2
ϑ	5.1		

3.4 Results and discussions

The constraint minimization problem (4) does not yield a reasonable solution. Due to the viscoelastic effect, this model has an upper bound for the final take-up velocity[10] and this upper bound value depends on $v(L) \leq v_0 + \int_0^L \frac{1}{\lambda(T,\varphi)} dz$.

Since the fluid characteristic relaxation time depends on the temperature and crystallization profiles, the upper bound value also depends on these two profiles. The temperature and crystallization profiles vary with respect to parameters such as the air velocity, air temperature and etc. Hence the upper bound of the final take-up velocity also varies with respect to parameters. Therefore, one can expect that after a few iterations the optimal control problem (4) yields the upper bound which is lower than the prescribed take-up velocity. In other words, it is not possible to generate an optimal solution based on the cost functional (3a). Fig. 3 visualizes the sensitivity of the final take-up velocity with respect to the parameters, depending on the initial guess for the stress. From this, one can see that depending on the parameter values, the final take-up velocity has an upper bound. Further, one can observe, when temperature close to 60°C, the upper bond of the take-up velocity is below $65ms^{-1}$ whereas, it is below $50ms^{-1}$, when temperature close to 50°C. This provides evidence that final take-up velocity reaches to upper bound depending on other parameters. Therefore, it is not possible to consider (3a) as a cost funational.

By introducing the fiber length L as a new control variable (cost functional (3b)) we overcome these difficulties. Now in each iteration step, the upper bound also increases since it depends on the fiber length too.

Since, fiber length is introduced as a control variable, changing the fiber length, upper bound of the take velocity can be changed.

Fig. 4 shows the spinline velocity, temperature, crystallinity index, air velocity and air temperature profiles initially and after the optimization process for the cost functional . The corresponding cost functional J_2 is shown in Fig. 5 for two different tolerance values (10^{-2} and 10^{-3}).

Table 2: Summary of the parameters.

Parameter	Current	Optimal
Final Temperature $°C$	93.21	52.58
Fiber Length L m	1.00	1.32
Extrusion velocity v_0m/s	16.67	13.00
Crystallization starts at cm (from the spinneret)	24.00	19.00
Maximum crystallization at cm (from the spinneret)	71.5	62

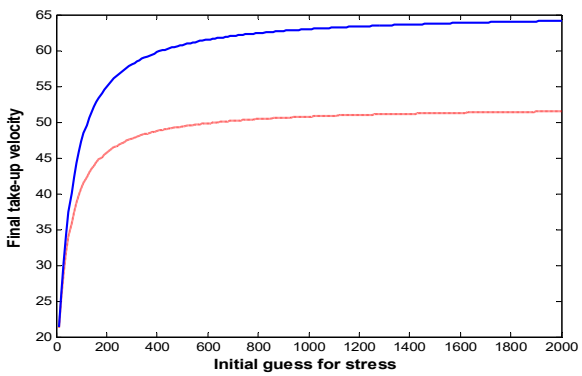

Fig. 3: Sensitivity of the final take-up velocity with respect to parameters, depending on the initial guess for stress. Solid: final temperature close to 60°C, Doted: final temperature close to 50°C

It can be noticed that in an optimal state the temperature at the take-up point is close to $52°$ C which is below the fiber solidification point. Hence one can expect that the polymer solidifies rapidly at this stage. The extrusion velocity drops from 16.67 m/s to 13.00 m/s. The air temperature profile is close to the reference temperature. The air velocity shows a high value just near the spinneret exit point. After that it is almost close to the initial profile. This means that just after the spinneret we need to arrange high air circulation which rapidly increases the cooling process. In the optimal state the fiber length reaches 1.32 m from its initial length of 1 m. One can observe that the crystallization process starts earlier than the initial stage and that it also reaches its maximum rate earlier than the initial state. A comparison of the control parameters initially and after the optimization process is summarized in Tab. 2.

4 Conclusions

We studied the optimization problem for flow induced crystallization viscoelastic melt spinning processes with respective the processing conditions. The aim was to maximize the outflow as well as to control the temperature profile (in order to get the final temperature below the fiber solidification point). Defining the cost functional we converted this problem into a constrained optimization problem and derived the first order optimality system. For the numerical simulation, we proposed the steepest decent algorithm based on the adjoint variable method.

It can be seen that the constrained optimization problem (4) does not produce the solution. From this we can extend the results obtained from[10] for the flow induced crystallization model too. It has been noticed that

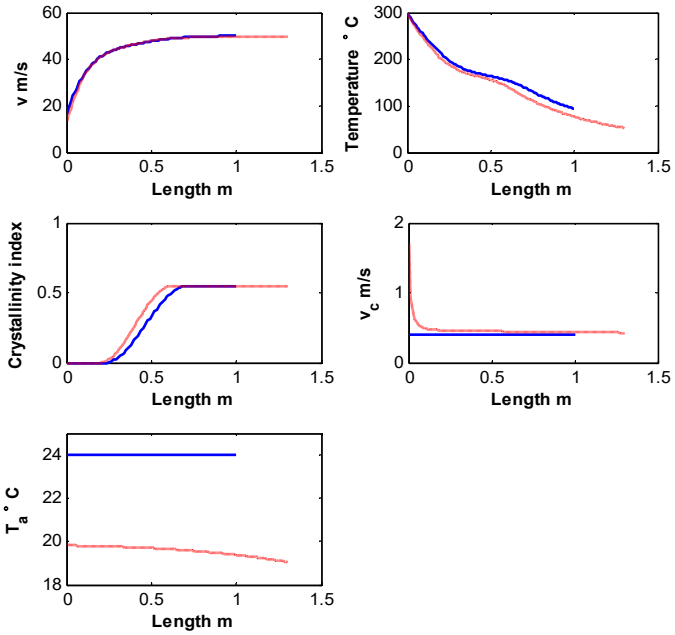

Fig. 4: For the J_2 cost functional: Spinline velocity, temperature, crystallinity index, air velocity and air temperature profiles, Solid: initial profile, Dotted: after optimization.

in an optimal state the temperature at the take-up point is close to $52°$C. Furthermore, we observed that the air velocity is high near the spinneret and that beyond that it is almost close to the initial profile, and the air temperature profile is more or less close to the reference temperature. The crystallization process also starts at early stage and reaches the maximum level before the initial profile. Clearly, this approach is successful with regard to cost.

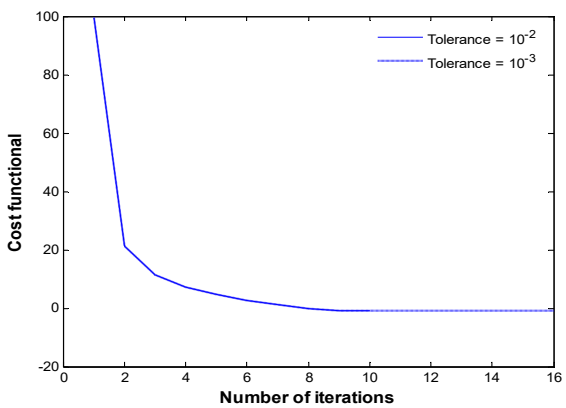

Fig. 5: Cost functional J_2

References

[1] A. Patnaik, R.D. Anandjiwala. An optimized melt spinning process to increase the productivity of nanofiber materials. *Journal of Industrial Textiles*, 2016, **45**(5): 1026–1037.

[2] A. Blim, L. Jarecki, S. Blonski. Modeling of pneumatic melt drawing of polypropylene super-thin fibers in the laval nozzle. *Bulletin of the Polish Academy of Sciences Technical Sciences*, 2014, **62**(1): 43–54.

[3] T. Goetz, S. S. N. Perera. Optimal control of melt-spinning processes. *Journal of Engineering Mathematics*, 2010, **67**(3): 153–163.

[4] H. R. H. Brnig., D. Blechschmidt. High filament velocities in the underpressure spunbonding nonwoven process. *International Fiber Journal, December*, 1997, 129–134.

[5] K. Ito, Ravindran, S. S. Optimal control of thermally convected fluid flows. *Siam Journal on Scientific Computing*, 1998, **19**(6): 1847–1869.

[6] S. Kase, T. Matsuo. Studies on melt spinning. i. fundamental equations on the dynamics of melt spinning. *Journal of Polymer Science Part A Polymer Chemistry*, 1965, **3**(7): 2541–2554.

[7] C. T. Kelley. *Iterative Methods for Optimization*. SIAM,1999.

[8] H. P. Langtangen. Derivation of a mathematical model for fiber spinning. 1997.

[9] S. S. N. Perera. Phase-space analysis of melt spinning processes. *Nihon Reoroji Gakkaishi*, 2008, **36**(4): 161–166.

[10] S. S. N. Perera. Viscoelastic effect in the non-isothermal melt spinning processes. *Applied Mathematical Sciences*, 2009, **3**(4): 177–186.

[11] L. F. Shampine, M. W. Reichelt. *The MATLAB ODE Suite*. Society for Industrial and Applied Mathematics, 1997.

[12] B. Younes, A. Fotheringham, H. M. E.-D. et al. Factorial optimization of the effects of melt-spinning conditions on biodegradable as-spun aliphatic-aromatic copolyester fibers iii. diameter, tensil properties and thermal shrinkage *Journal Applied Polymer Science*, 2014, **122**(2): 1434–1449.

[13] A. Ziabicki. Fundamentals of fiber formation. *Wiley-Interscience, New York*, 1976,